Calculation of ion energy distributions from radio frequency plasmas using a simplified kinetic approach

Martin Misakian[a] and Yicheng Wang
Electricity Division, National Institute of Standards and Technology, Gaithersburg, Maryland 20899-8113

(Received 23 November 1999; accepted for publication 18 January 2000)

Using an elementary kinetic approach, a procedure is described for calculating ion energy distributions (IEDs) from radio frequency (rf) plasmas. The calculated distributions, which are in the form of histograms, are used to fit experimental argon and CF_3^+ IEDs measured in a Gaseous Electronics Conference rf reactor modified to operate in a pulsed inductively coupled mode. Given the average plasma potential profile and its time dependence, the calculation incorporates a number of parameters used in more comprehensive treatments of the problem to determine the shape of the IED. The reverse calculation that determines the average potential profile, given an experimental IED, cannot be uniquely done, but some insights may be gained in some cases if a sufficient number of plasma related parameters are known, e.g., the shape and amplitude of the rf modulation. The results of the calculation indicate that argon ions forming the IEDs during the bright (H) mode come nearly exclusively from a presheath region that extends far into the interior of the plasma. The calculations also suggest that the CF_3^+ ions forming the IEDs observed during the dim (E) mode may preferentially come from near the ''edge'' of the bulk plasma. Possible significances of this difference are noted. © *2000 American Institute of Physics.* [S0021-8979(00)06908-5]

I. INTRODUCTION

Because ion bombardment plays a crucial role in etching discharges, considerable effort has been devoted to understanding how ion energy distributions (IEDs) are controlled by the plasma potential and associated electric field in the sheath region in various radio frequency (rf) plasmas. For example, Miller and Riley have investigated the physics of the plasma sheath using a semianalytic model,[1] and Hoekstra and Kushner[2] have studied IEDs in inductively coupled plasmas (ICPs) with chlorine-containing gas mixtures using a ''hybrid plasma equipment model'' linked with a ''plasma chemistry Monte Carlo simulation.'' Wild and Koidl[3] studied IEDs in capacitively coupled plasmas which exhibit multiple peaks. They explained the IED features by modeling the ion transport through rf modulated collisional sheaths. However, the shapes of observed IEDs are often explained only qualitatively. For example, Wang and Olthoff[4] attributed variations in IEDs observed in Ar, N_2, O_2, and Cl_2 plasmas to varying degrees of rf modulation across the ground sheath. This explanation is overly simplistic because the electric field in the presheath region may significantly influence the ion energy distributions.

Given the average potential profile and its time dependence, in this article we describe a procedure using an elementary kinetic model for calculating the shape of the IEDs from rf plasmas. The calculation leads to the construction of histograms that are used to fit experimentally determined IEDs. While the calculations incorporate some parameters included in more comprehensive treatments of the problem, e.g., the phase of the electric field, Maxwellian velocity distributions, charge exchange collisions, mean free paths, and points of origin of ions in the plasma,[2,3,5,6] the elementary approach may make the connection between these parameters and the IEDs measured more transparent. The experimental IEDs considered in this article are obtained from a 13.56 MHz argon plasma in a Gaseous Electronics Conference (GEC) rf reference reactor[7] modified to operate in a pulsed inductively coupled mode.[8,9] Given an experimentally determined IED, it may be possible to construct some features of the potential profile in the sheath and presheath[10] regions, although the uniqueness of the profile cannot be assured, as is discussed when considering a CF_3^+ IED.

II. EXPERIMENTAL APPARATUS

Plasmas were generated in a GEC rf reference reactor whose upper electrode was modified to house a five-turn planar rf-induction coil behind a quartz window to produce inductively coupled discharges.[8] The ion sampling arrangement is the same as that used to study inductively coupled plasmas generated in CF_4 under continuous excitation.[11] Ions are sampled through a 10 μm diam orifice in a 2.5 μm thick nickel foil that was spot welded into a small counterbore in the center of the bottom grounded electrode of the reactor. For IED measurements, the ions that pass through the orifice are accelerated and focused into a 45° electrostatic energy selector. After being selected according to their energy, the ions enter a quadrupole rf mass spectrometer where they are selected according to their mass-to-charge ratio and detected with an electron multiplier. The resolution of the electrostatic analyzer was fixed at a value of 1 eV, full width at half maximum, and the uncertainty of the energy scale is estimated to be less than ± 1 eV.

For pulsed operation of the reactor, the rf power to the inductive coil was supplied by a rf amplifier with its input

[a]Electronic mail: misakian@eeel.nist.gov

connected to a wave form synthesizer operating at 13.56 MHz. A master gate pulse generator with a variable pulse repetition rate and duty cycle was used to gate the rf output and to synchronize all time-resolved measurements. Time-resolved IED measurements were made by gating the digital ion counting pulses from the electron multiplier. The gating pulse, which could be varied in width, was synchronized to the master gate pulse generator through a variable digital delay generator.

When operated in the pulse mode, the plasma can exist in two states: a dim or E mode with characteristics of a capacitively coupled plasma, and a bright or H mode with characteristics of an inductively coupled plasma. When the rf energy is applied to the induction coil, the plasma for our conditions initially begins in the E mode and then undergoes a transition to the H mode.[9] Ion energy distributions measured during the E mode and H mode are considered for fitting using the model calculation method described in Sec. III.

III. KINETIC MODEL

We begin by considering an average electric potential in the sheath and presheath regions of the plasma that is a function of position. The approximation of one dimensional ion motion allows us to express the average potential as a function of the coordinate x, i.e., $V(x)$, and the negative gradient of $V(x)$ yields the average electric field, $E(x)$. Because the wavelength of the rf modulation ($\sim 22\,\mathrm{m}$) is much greater than any relevant experimental dimension ($<0.1\,\mathrm{m}$), we make the assumptions that the electric field in our model is quasistatic[12] and that the time variation of the electric field and plasma potential can be incorporated as a multiplicative factor. That is,

$$V(x,T)=V(x)[1+\alpha\sin(\omega T+\Phi)], \tag{1}$$

and

$$E(x,T)=E(x)[1+\alpha\sin(\omega T+\Phi)], \tag{2}$$

where $\alpha V(x)$ is the amplitude of the rf modulation of the potential, ω is $2\pi f$ where f is the frequency, Φ is the phase of the potential or electric field when the ion enters the electric field, and T is the time at some instant (see below) during the time variation of the potential and electric field.

The force on an ion is

$$F=m\frac{dv}{dt}=qE(x)[1+\alpha\sin(\omega T+\Phi)], \tag{3}$$

where m and q are the mass and charge of the ion, respectively.

Equation (3) is solved in an approximate fashion using a step-by-step procedure during which the force is held constant as the ion moves a short prescribed distance toward the grounded bottom electrode of the GEC cell. The solution for the final velocity, v, after the ion travels some distance (taken below as Δx) is found by integrating Eq. (3), i.e.,

$$v=v_o+\frac{q}{m}E(x')[1+\alpha\sin(\omega T+\Phi)]t, \tag{4}$$

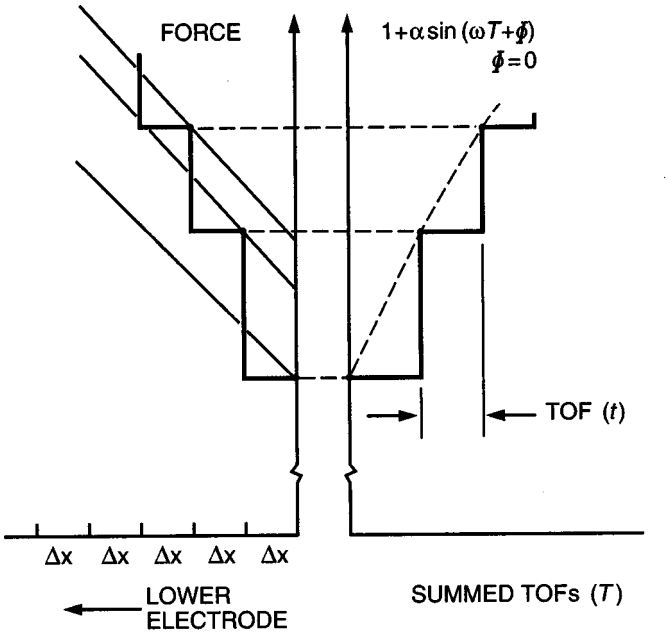

FIG. 1. Schematic view (not to scale) showing how the time dependent multiplicative factor in the equations is updated through the summation of TOFs, which together with the position of the ion (x) establishes the magnitude of the force for the next interval, Δx. A linear electric field is assumed here.

where v_o is the initial velocity, $E(x')[1+\alpha\sin(\omega T+\Phi)]$ is held constant, and t is the time of flight (TOF) with the initial value of t being taken as zero. T is the sum of the TOFs for traveling all of the earlier Δx intervals. A prime was added to the x value to indicate that it was held constant during the integration.

Noting that $v=dx/dt$ for the Δx interval under consideration, we can integrate both sides of Eq. (4) to obtain an expression for t as the ion travels the distance Δx,

$$\Delta x=v_o t+\frac{q}{m}E(x')[1+\alpha\sin(\omega T+\Phi)]\frac{t^2}{2}. \tag{5}$$

Equation (5) is a quadratic equation for t and is readily solved using the quadratic formula. The value of t is then used in Eq. (4) to determine v and this value of v becomes the initial velocity, v_o, for the next interval. The value of Δx is subtracted from the remaining distance to the grounded electrode to obtain the x' for the next interval and, as noted above, the value of t is added to the previous TOFs to obtain the new T. The ''updated'' product of $qE(x')[1+\alpha\sin(\omega T+\Phi)]$ becomes the force that is held constant for the next interval. Figure 1 illustrates schematically the step-by-step procedure. The process is repeated until the total distance traveled by the ion is equal to the assumed sheath/presheath width. The final velocity when the ion reaches the grounded bottom electrode is used to calculate the kinetic energy. By making Δx sufficiently small, it becomes possible to capture with adequate accuracy the magnitude of the changing force acting on the ion as it travels to the grounded electrode.

The model incorporates the effects of collisions, which are not included in the above equations, by considering the

mean free path (mfp) of the ions during the calculation of the kinetic energies (see below). While we can anticipate that the mfp for argon ions will be mainly influenced by the large cross section for charge exchange, the mfp is used as a fitting parameter during the process of matching the calculated and measured IEDs. In gases where charge exchange or other collision processes that lead to the thermalization of the ion are not dominant, the approach described below would have to be modified because ions that travel to the grounded electrode are assumed to begin with thermal energies.

To construct histograms for fitting experimentally obtained IEDs, a computer program is used to calculate the kinetic energies of ions reaching the grounded electrode using the step-by-step procedure described above.

(1) The calculation assumes a given average electric potential profile (and associated electric field) that is amplitude modulated sinusoidally at a frequency of 13.56 MHz.
(2) Ions are created by electron impact ionization and charge exchange collisions.
(3) Ions initially have a range of thermal velocities given by the Maxwellian velocity distribution.
(4) Ions enter the field at a uniform rate in space and time for different phases, Φ, of the electric field.
(5) Ions originate uniformly from a range of starting points, X_o, where there exist both thermal ions and an electric field directed toward the grounded electrode.
(6) Because the mfp of an ion will change as its velocity increases, an average or ''effective'' mfp is assumed for the calculations (see below).
(7) Uniform temperature and pressure profiles are assumed to exist along the ion trajectory.
(8) The number of ions that arrive at the bottom plate are weighted by the function,

$$W\mathrm{T}=\exp\left(-\frac{X_o}{L}\right)\exp\left(-\frac{mv_{\mathrm{T}}^2}{2k\mathrm{T}}\right), \tag{6}$$

where the first exponential is the mfp distribution with an average mfp value of L, and the second exponential is (within a constant) the Maxwellian velocity distribution, with k equal to the Boltzmann constant, T (not in italics) is the absolute temperature, and v_{T} is the thermal velocity of the ion as it begins its movement in the electric field toward the bottom electrode. For each ion arriving at the grounded electrode with energy in the interval E to $E+\Delta E$, an entry equal to the magnitude of WT is made in the appropriate energy bin to construct the IED histogram. The width of the energy bin used in the calculations described below is 0.2 eV.

IV. AVERAGE ELECTRIC POTENTIALS AND Ar^+ ION ENERGY DISTRIBUTIONS

To calculate the IED for argon ions from an argon plasma, we make use of the average plasma potential profile measurement by Miller *et al.*[8] in an inductively coupled continuous (not pulsed) argon plasma produced in a GEC rf reference cell and potential measurements 1.2 cm above the grounded lower electrode in a GEC cell at the National Institute of Standards and Technology (NIST).[13] The power and pressure during the Miller *et al.* measurements were 150 W and 1.33 Pa (10 mTorr), respectively. The NIST measurements were performed as a function of pressure, but power information was not reported. Figure 2 shows a portion of the Miller *et al.* profile which extends from 0.1 cm above the grounded electrode (the lowest point measured) to a height of 1.9 cm.[14] The potential flattens at about 1.9 cm and argon ions in the plasma can from this point contribute to the calculated IEDs. The measurements of Miller *et al.* are fitted with a potential of the form,

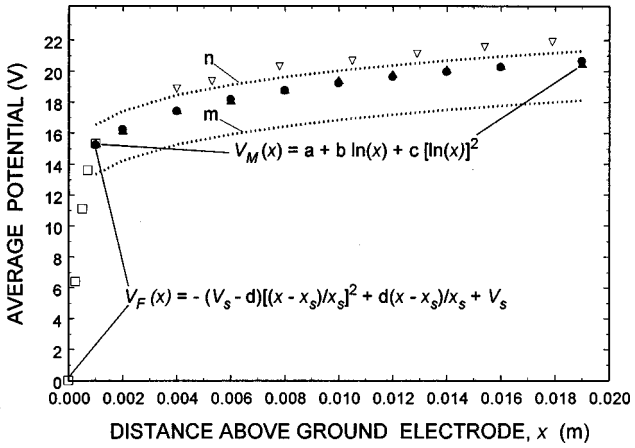

FIG. 2. Average potential profile after Miller *et al.* (Ref. 8) (▲). The triangles are fitted with the function $V_M(x)$, which is used to determine the electric field along the x axis between x_s and $x=0.019$ m. Predictions of $V_M(x)$ are indicated by closed circles (●). The open squares (□) represent several points predicted by $V_F(x)$, where $V_F(x)$ and the gradient of $V_F(x)$ were made to match the corresponding values for $V_M(x)$ at x_s. The open inverted triangles (▽) are the measurements of Schwabedissen *et al.* (Ref. 13), but they were not used in the calculations. Profiles m and n are used to calculate the IEDs in Fig. 3 and in the inset in Fig. 4, respectively.

$$V_M(x)=a+b\ln\left(\frac{x}{D}\right)+c\left[\ln\left(\frac{x}{D}\right)\right]^2, \tag{7}$$

where a, b, and c are equal to 32.77, 3.743, and 0.175, respectively, in units of volts. D is equal to 1 m and the values of x are expressed in units of meters.

The average potential between the bottom electrode and where it meets the Miller *et al.* potential is modeled with a potential of the form used by Fivaz *et al.*[15] for a linear electric field,

$$V_F(x)=-(V_s-d)\left(\frac{x-x_s}{x_s}\right)^2+d\frac{(x-x_s)}{x_s}+V_s, \tag{8}$$

where V_s is the potential value where $V_F(x)$ and $V_M(x)$ meet at a distance of x_s above the grounded electrode. Figure 2 shows the meeting point, x_s, as being equal to 0.1 cm but, as discussed later, better matches between the calculated and measured IEDs can be obtained by adjusting the value of x_s. The parameter d is used to match the gradient of $V_F(x)$ with that of the Miller *et al.* potential at $x=x_s$.[16] The negative gradients of $V_M(x)$ and $V_F(x)$ are the average electric fields that exert a force on the ions as they travel through the regions $x_s \leqslant x \leqslant 1.9$ and $0 \leqslant x < x_s$ cm respectively.

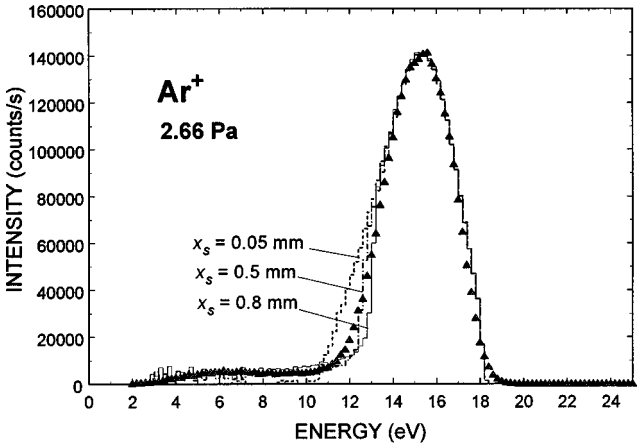

FIG. 3. Ar^+ IED measured during the bright mode (H mode) at 2.66 Pa (20 mTorr) and calculated energy distributions. The three histograms represent candidate matches between calculations and the measured IED assuming different values of x_s where $V_F(x)$ and $V_M(x)$ are joined. The peak heights of the histograms were made equal to that of the measured IED.

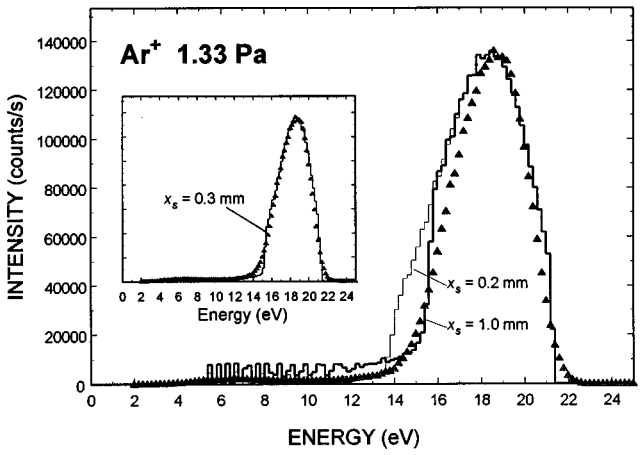

FIG. 4. Ar^+ IED measured during the bright mode at 1.33 Pa (10 mTorr) and two calculated energy distributions assuming different values of x_s. The peak heights of the histograms were made equal to that of the measured IED. The inset shows good agreement between the calculated and measured IEDs if a flatter average potential profile is used in the extended presheath region.

The open triangles in Fig. 2 show a portion of a potential profile measured in the NIST GEC reactor when the power and argon pressure were 84 W and 1.33 Pa, respectively.[13] These data were not considered for use in the model calculations because of their more limited range compared to the Miller *et al.* results.

Figure 3 shows an argon IED from an argon plasma in the NIST GEC rf cell measured during the bright mode of the discharge. During the measurements, the pressure was 2.66 Pa (20 mTorr) and the peak power[17] was 200 W. To perform the calculations, $V_M(x)$ was multiplied by a scaling factor of 0.876 to match the NIST potential measurements at $x=1.2$ cm for the same pressure. After multiplying by the scaling factor, the values of a, b, and c [Eq. (7)] become 28.70, 3.278, and 0.1528, respectively (Fig. 2, profile m). The same scaling factor was also applied to $V_F(x)$. The significance of using a multiplicative scaling factor and not an additive constant to $V_M(x)$ is discussed later. Figure 3 also shows the results of three calculations assuming different values of x_s where $V_M(x)$ and $V_F(x)$ are joined. Assuming $x_s=0.05$ mm ($d=0.251$) leads to the elimination of most ions in the low energy tail of the IED. The results for $x_s=0.8$ mm ($d=1.098$) and $x_s=0.5$ mm ($d=0.955$) are similar although, while not obvious from Fig. 3, a better match is obtained for the low energy tail when $x_s=0.8$ mm. A slightly improved match is obtained with the main portion of the IED (>12 eV) by using $x_s=0.5$ mm.

The IED calculations assume an average mfp (L) of 0.52 cm, a temperature of 600 K,[18] and ions that originate from 1.9 to roughly 0.01 cm above the grounded electrode contribute to the energy distribution. The value of Δx was 9.5×10^{-5} cm and the separation in X_o values was 26 μm for most of the calculation, although the main features of the IED (between ~12 and 18.1 eV) could be determined with values twice as large.[19] The calculation takes into account values of the phase, Φ, ranging from 0° to 358° in 2° steps, and assumes the amplitude of the rf oscillations of the plasma potential, αV (1.9 cm), is equal to 0.75 V which is similar to a previously reported amplitude in an argon plasma.[20] The calculated histogram is not highly sensitive to small changes in the value of α V (1.9 cm). The thermal velocities, v_T, considered for the weighting function, WT, increased from zero in 100 m/s steps to a value for which WT was less than 0.0015.

Assuming that the gas pressure measurement accurately reflects the pressure over the path taken by the ion, we use the approximate relation between the mfp, L, the gas density, n, and the cross section,[21] σ, i.e., $L\approx1/n\sigma$, to obtain an estimate of the average cross section. For the given conditions, $\sigma\approx5.9\times10^{-15}$ cm^2, which is consistent with an $Ar+Ar^+$ charge-transfer cross section, but near the upper limit for the range of published cross section values, i.e., between $\sim6\times10^{-15}$ and $\sim3.5\times10^{-15}$ cm^2 for ion kinetic energies of $1-\sim20$ eV.[22]

Figure 4 shows an argon IED recorded in the NIST GEC reactor during the bright mode at a pressure of 1.33 Pa (10 mTorr). For this case, the NIST potential measurement at $x=1.2$ cm above the grounded electrode for the same pressure suggested that the potential profile [Eqs. (7) and (8)] be scaled upward by a factor of about 1.045. This leads to a potential at $x=1.9$ cm of 21.6 V, which in turn leads to a maximum ion kinetic energy near 21.6 eV, ignoring the instrumental spreading of the IED. The maximum kinetic energy in Fig. 4 is near 21.3 eV, which is slightly lower. Therefore, to fit the IED in Fig. 4, the scaling factor was chosen so that the maximum kinetic energy from the calculation would match the IED data, i.e., the scaling factor was made 1.03, raising the average potential at $x=1.9$ cm to 21.3 V. For this case, the values of a, b, and c are 33.76, 3.855, and 0.1797, respectively.

Figure 4 also shows two calculated IEDs assuming x_s values of 0.2 mm ($d=0.793$) and 1.0 mm ($d=1.332$). While not clear from Fig. 4, the histogram for $x_s=0.2$ mm predicts a low intensity of ions in the low energy tail,

roughly consistent with the data, but overestimates the number of ions with energies $\sim 14 - \sim 18$ eV. The histogram for $x_s = 1.0$ mm provides a somewhat better fit over the higher energies, but overestimates the number of ions in the low energy tail.

Ions that contribute to the calculated IEDs are assumed to come from 1.9 to ~ 0.004 cm ($x_s = 0.2$ mm) and from 1.9 to ~ 0.002 cm ($x_s = 1$ mm) above the grounded electrode. The peak power was again 200 W and a mfp of 0.635 cm was assumed for the calculations. The amplitude of the rf oscillations of the plasma potential was taken to be 0.4 V although the calculation again is not sensitive to small changes in this value. The earlier remarks regarding v_T, WT, Φ, the value of Δx, and the separation in X_o values apply. Because no information was available regarding the temperature at the reduced pressure during measurements of the IED, it was assumed to be 450 K. For this temperature, the average cross section is $\approx 7.3 \times 10^{-15}$ cm^2, which is somewhat high compared to the published values for $Ar + Ar^+$ charge exchange.

The results in Fig. 4 indicate that the main portions of the calculated IEDs ($x_s = 0.2$ mm, $x_s = 1$ mm) are both too wide compared to the measured IED. A method for reducing the width of the calculated IEDs is to decrease the slope of the potential profile in the extended presheath region. This result can be readily shown using simple graphical analyses with potential profiles that have different slopes. The inset in Fig. 4 shows the results of a calculation for which the potential in the extended presheath has been made slightly flatter than the Miller *et al.* profile (i.e., $a = 31.89$, $b = 3.278$, $c = 0.1528$; Fig. 2, profile n), $x_s = 0.3$ mm, $d = 0.7987$, $L = 0.6$ cm, and T = 400. The approximate collision cross section at 1.33 Pa for the given temperature and mfp is about 6.9×10^{-15} cm^2, which is again somewhat high compared to published charge exchange cross sections for argon ions. The amplitude of the rf oscillations was 0.4 V and ions were assumed to come from 1.9 cm to roughly 60 μm above the grounded electrode. For these conditions, good agreement is obtained between the calculated and measured IEDs. As will be discussed later, the earlier difficulty in obtaining a satisfactory fit to the measured IED at 1.33 Pa can be traced back to the method used in scaling the Miller *et al.* potential profile. The flatter profile that was chosen is also discussed.

V. CF_3^+ ION ENERGY DISTRIBUTION AND CANDIDATE AVERAGE POTENTIAL PROFILE

During the course of developing equations for the argon IEDs, it was observed that bimodal IEDs could occur if a linear electric field [Eq. (8)] with a short presheath region was assumed for the calculations. For this case, the extended ''presheath'' in Fig. 2 for argon is replaced by a potential profile that has a short presheath followed by an extended region that is flat, i.e., the electric field in the bulk of the plasma is assumed to be negligible. Bimodal distributions have been observed for CF_3^+ IEDs during the dim mode of a CF_4/Ar plasma[9] and thus the appropriateness of a linear electric field for this case was investigated.

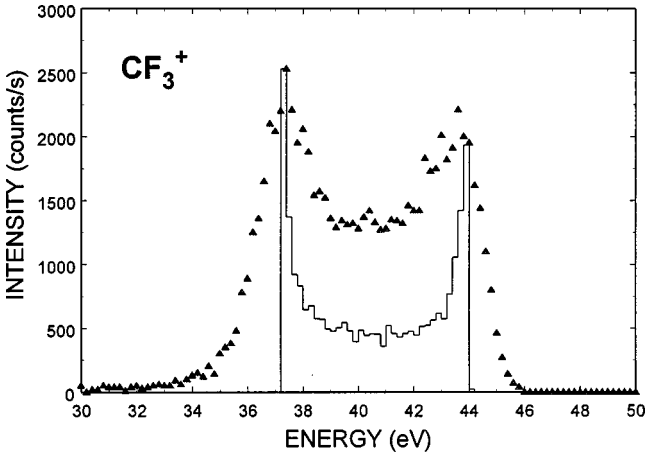

FIG. 5. CF_3^+ IED measured during the dim mode at 2.66 Pa (20 mTorr) and calculated energy distribution assuming ions with thermal energies come from a single point near the edge of the bulk plasma. The left peak height of the histogram was made equal to that of the measured IED.

A significant difference in the formation of CF_3^+ and Ar^+ IEDs is the absence of charge exchange collisions involving CF_3^+, or other collision processes (involving CF_3^+) with cross sections having a comparable order of magnitude. This leads to simplification of the calculation of the IEDs, namely, ignoring collisions in the sheath region because of the relatively large mfp (L) and short distances, X_o's, that ions travel under the influence of the electric field. Assuming a collisionless sheath,[1] the mfp distribution, which is a factor in Eq. (6), is dropped when the calculations are performed.

Figure 5 shows the CF_3^+ IED from a 50%CF_4/50%Ar plasma recorded during the dim mode at a pressure of 2.66 Pa and when the power deposited in the plasma was much less than the 280 W peak power. Further details of the IEDs that were measured as well as optical emissions from the pulsed inductively coupled plasma are described elsewhere.[9] A candidate average potential profile was examined by assuming a linear electric field and a value for the sheath potential suggested by the average kinetic energy of the IED, which is near 40.5 eV. The histogram in Fig. 5 was constructed assuming that the average potential profile is given by Eq. (8), with $d = 1$ V, $V_s = 40.55$ V, $x_s = 0.236$ cm, and T = 500 K. The amplitude of the rf modulation of V_s was assumed to be 32 V and all of the ions in the IED started from a single point, $X_o = 0.2364$ cm. Except for V_s, the selection of the above parameters was arbitrary. In general, for a given amplitude of modulation and V_s value, increasing x_s makes the calculated bimodal distribution narrower because, as expected, the ions require more time to cross the sheath and tend toward the average kinetic energy. Conversely, decreasing x_s increases the width of the calculated bimodal distribution within limits set by the amplitude of the rf plasma oscillations.

Figure 6 illustrates how the calculated energy distribution for the measured IED in Fig. 5 can be improved. To obtain the more realistic histogram in Fig. 6, the presheath region was extended a small amount by increasing d in Eq. (8) to 10 V, and ions in the calculated IED were allowed to come from a narrow range of distances, namely, 0.190 cm

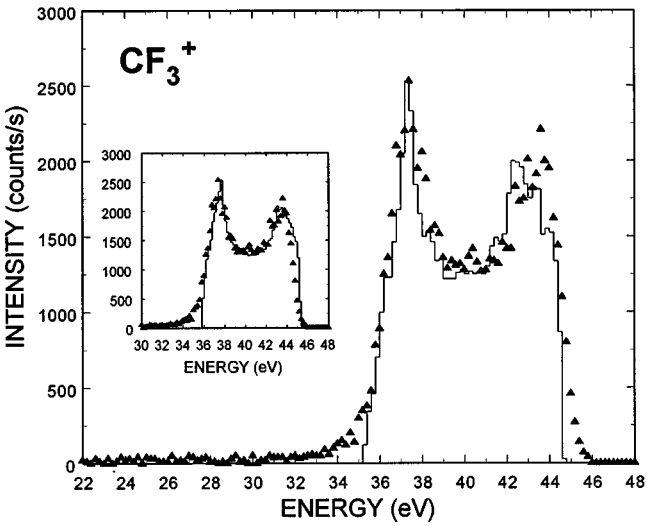

FIG. 6. CF_3^+ IED from Fig. 5 and calculated energy distribution assuming ions with thermal energies come from a range of distances near the edge of the bulk plasma. The left peak height of the histogram was made equal to that of the measured IED. The inset shows a comparison of the a measured and a calculated IED assuming an unrealistic value for the sheath width, x_s.

$\leqslant X_o \leqslant 0.235$ cm. Other parameters used in the calculations were T=500 K, $x_s=0.215$ cm, $V_s=40.5$ V, and rf modulation amplitude equal to 35.4 V.

The inset in Fig. 6 shows a similar realistic appearing calculated IED obtained when $d=10$ V, T=400 K, $V_s=41.3$ V, 0.0354 cm$\leqslant X_o \leqslant$0.0418 cm, rf modulation amplitude equal to 7.8 V, and an unrealistic value of the sheath width for the dim mode, $x_s=0.04$ cm.

VI. DISCUSSION

A. Argon IED (2.66 Pa)

The very good agreement between the measured and calculated ($x_s=0.5$ and 0.8 mm, respectively) IEDs in Fig. 4 can be regarded as fortuitous to some degree because of the assumptions that go into the modeling, including the method for scaling the Miller *et al.* potential, and because there likely exist uncertainties in the Miller *et al.* and NIST potential measurements. In addition, the power during the Miller *et al.* potential measurements was 150 W, whereas the NIST IED measurement was recorded at a peak power of 200 W. Yet, it is noteworthy that most of the average potential profile used for the calculations was obtained by applying a simple scaling factor. The discrepancies between the measured and calculated IEDs near 13 eV correspond to the region where the adjusted (for NIST conditions) potentials V_M and V_F are joined and thus it is not surprising considering the uncertainties that could exist in this region.

Several other observations can be made from the results shown in Fig. 3.

(1) To calculate realistic IEDs, it is necessary to take into consideration ions that come from a range of distances above the grounded electrode. As seen from the Miller *et al.* profile measurement, the electric field in an inductively coupled plasma can extend far into the interior of the plasma and some ions from this region will contribute to the IED. The maximum kinetic energy will correspond to the maximum plasma potential if experimental rounding of the IED is ignored. It is noteworthy that most of the IED is composed of ions that come from an extended ''presheath.''

(2) Because the average plasma potential profile used in the calculations was largely taken from the data recorded during a continuously excited inductively couple plasma, and the IED measurement was recorded during the bright mode of a pulsed inductively coupled plasma, the potential profiles for the two conditions (continuous and pulse/bright modes) apparently are similar. However, it should be noted that because the scaling factor used to obtain the average potential profile was multiplicative and less than unity (0.876), the profile was made flatter than the Miller *et al.* profile, $V_M(x)$. If the scaling had been accomplished by using an additive constant to $V_M(x)$, the slope of the profile would have remained unchanged, and the main portion of the calculated IEDs would have been too wide. Calculations not shown confirm this observation.

(3) From an examination of the average potential profile for the NIST calculation (not shown), the disappearance of significant numbers of argon ions near 3 eV in the measured IED indicates that the $Ar+Ar^+$ charge exchange collisions cease to occur in significant numbers at a height of about 0.01 cm above the grounded electrode.

(4) The approximation of a linear electric field very close to the grounded electrode is supported by the agreement between the IED and calculation in this region, i.e., along the low energy ''tail'' of the IED. The same approximation in the region where the adjusted $V_F(x)$ and $V_M(x)$ meet is not as good.

(5) The value of x_s strongly influences the intensity of calculated ions in the low energy tail, i.e., the number of ions in the low energy tail decreases as x_s is made smaller.

(6) The histogram calculations are not highly sensitive to absolute temperature, but the temperature does significantly influence estimates of the average cross section.

(7) The alignment of the calculated and measured IED peak energies is sensitive to the choice of the mfp. Although not shown in Fig. 3, increasing or decreasing the mfp shifts the peak kinetic energy of the IED to higher or lower values, respectively.

(8) Knowledge of the gas temperature, density, and the cross sections for the predominant ion-atom collision processes provides a means for checking the consistency of the mfp assumed for the calculation. The slightly high cross section value for charge exchange estimated from the value of L used to match the calculated and measured IED at 2.66 Pa (and 1.33 Pa) is likely due to many simplifying assumptions that are incorporated into the model. For example, the approximate expression used to estimate the cross section, $\sigma \approx 1/nL$, assumes that the ions travel through a stationary background gas, whereas the background gas particles move with elevated thermal energies. Taking this motion into account would reduce

the numerator on the right-hand side of the expression, and the estimated cross section. Also, we may be overlooking some ions that undergo inelastic collisions, followed by collisions that lead to thermal ions, and that still contribute to the IED and the estimated cross section.

It should be noted that because the time variation of the plasma potential is in the form of a multiplicative factor, it can be readily modified to consider the effects of wave forms other than purely sinusoidal. For example, the effects of harmonics and their phase relation to the fundamental frequency can be investigated.

B. Argon IED (1.33 Pa)

The agreement between the measured and calculated IEDs at 1.33 Pa shown in Fig. 4 (excluding the inset) is only fair compared to the 2.66 Pa case. By increasing the mean free path in the calculations, better agreement could be obtained between the peak values, but the agreement of the high energy trailing edge of the histogram ($\gtrsim 19$ eV) would worsen. As noted earlier, the calculated IEDs are too wide. The problem is due, in part, to the use of a multiplicative scaling factor greater than unity to obtain the potential profile in the presheath region. The resulting increased slope of the profile contributes to the wider calculated IED as was noted earlier. The flatter presheath potential used to calculate the IED in the inset in Fig. 4, which shows good agreement with the measured IED, was obtained by adding a constant (3.19 V) to the presheath potential profile used for the 2.66 Pa calculations. This constant voltage raises the potential at $x_s = 1.9$ cm to 21.3 V which is consistent with the maximum kinetic energy of the measured IED. It thus appears that the slope of the average potential profile in the presheath region is the same at 2.66 and 1.33 Pa. Using a multiplicative scaling factor less than unity for the earlier 2.66 Pa calculation instead of adding a constant to the Miller *et al.* potential was a fortuitous choice. While the difference in slope between the Miller *et al.* potential profile and the ones used for obtaining favorable calculated IEDs at 1.33 and 2.66 Pa is not great (Fig. 2), the small difference does significantly affect the outcome of the calculations. We note that the adjusted profile (Fig. 2, profile n) is very close to the NIST measurements at the same pressure, but different power (Fig. 2, open triangles).

C. CF_3^+ IED (2.66 Pa)

The calculated IEDs in Figs. 5 and 6 illustrate once again the need to consider ion contributions to the energy distribution from a range of distances in the sheath/presheath regions. However, the results of the calculations are consistent with the view that the presheath region in the dim mode does not extend very far into the bulk plasma as in the case of the Ar^+ IEDs in the bright mode, i.e., most of the plasma appears to consist of an (average) equipotential region. The assumptions of a linear electric field and the absence of collisions in the sheath region also appear to be fair approximations.

The uniqueness of the average potential profile used in the calculation of the CF_3^+ IED cannot be assured as demonstrated by the two calculated histograms in Fig. 6. By scaling up or down the values of x_s and the rf modulation amplitude, for about the same value of V_s, and similarly scaling the range of X_o values comparable IEDs can be constructed. However, because of the strong influence of x_s and the amplitude of the rf oscillation on the calculated IED, knowledge of either parameter would allow an estimate of the other via the process of matching the calculated and measured IEDs. For example, if the amplitude of the rf oscillation is known from measurements, the determination of the sheath width, x_s, and thus the average potential profile will have less uncertainty when the calculated and measured IEDs are matched. Knowledge of the temperature also reduces the uncertainty in determining the average potential profile, although its influence is minor compared to those of the x_s and rf amplitude values.

As for the case of argon IEDs, the influence of wave forms other than purely sinusoidal can be readily investigated using the calculation method that has been described. In addition, a small modification in the calculation software for linear electric fields allows one to examine the effects of sheath width (x_s) variations, assuming its time dependence and phase relation relative to the plasma oscillations. However, it was not necessary to consider such variations for the results shown in Figs. 5 and 6.

VII. CONCLUSIONS

Given the average potential profile for a rf plasma and its time dependence, an elementary deterministic method has been described for calculating IEDs impinging on and exiting through the ground electrode of a GEC reactor. While the ''given'' potential profile provided by the Miller *et al.* measurements had to be modified slightly to conform to conditions in the NIST GEC reactor, the good agreement that could be attained between the calculated and measured IEDs provides support that the calculation method is basically sound assuming the approximations that were indicated. It is interesting to note that the slopes of the extended presheath profiles at 2.66 and 1.33 Pa in the argon plasmas are essentially the same, i.e., the electric fields acting on the ions are apparently the same. The reverse process of determining features of the average potential profile given a measured IED has much greater uncertainty associated with it, but some insights may be gained as knowledge of a number of parameters associated with the plasma increases, e.g., rf modulation amplitude, mean plasma potential, gas temperature, and gas density.

The calculations for the IEDs considered in this article give support to the assumption that linear electric fields very close to the ground electrode are a good approximation in GEC reactors. The results of the calculations are also consistent with the view that there can be significant differences between the average potential profiles in the bright and dim modes when the plasma is excited in a pulsed fashion. In the bright mode (inductive coupling) the ''presheath'' extends far into the interior of the plasma as previously reported[8] for

continuous plasma excitation whereas in the dim mode (capacitive coupling) the penetration of the electric field into the bulk plasma is relatively nil. A consequence of the first observation is that ions in the IEDs come from a range of points (X_o's) extending well into the plasma; most of the ions in the IED come from the extended presheath. A consequence of the latter observation is that the starting points of the ions that travel to the grounded electrode may be preferentially from a narrow range near the ''edge'' of the bulk plasma. These differences may be of interest when pulsed inductively coupled plasmas are considered for plasma processing. For example, if the density profile of ions is not uniform throughout the plasma[23] and there are multiple ion species, there could be differences in the predominant ion or mix of ions in the flux impacting a target wafer, depending on the mode of plasma excitation. In addition, estimates of the relative abundances of ions in the bulk plasma from IED measurements performed during the dim mode may be affected.

The simplicity of the calculation method has its obvious limitations. For example, it does not consider ions that might approach a substrate in directions other than normal[6] and it cannot predict flux densities. The method does allow investigation of candidate potential profiles that might yield IEDs with shapes desirable for etching purposes, as reported recently by Wendt *et al.*[24]

[1] P. A. Miller and M. E. Riley, J. Appl. Phys. **82**, 3689 (1997).
[2] R. J. Hoekstra and M. J. Kushner, J. Appl. Phys. **79**, 2275 (1996).
[3] C. Wild and P. Koidl, J. Appl. Phys. **69**, 2909 (1991).
[4] Y. Wang and J. K. Olthoff, J. Appl. Phys. **85**, 6358 (1999).
[5] E. Kawamura, V. Vahedi, M. A. Lieberman, and C. K. Birdsall, Plasma Sources Sci. Technol. **8**, R45 (1999).
[6] D. Field, D. F. Klemperer, P. W. May, and Y. P. Song, J. Appl. Phys. **70**, 82 (1991).
[7] P. J. Hargis, Jr. *et al.*, Rev. Sci. Instrum. **65**, 140 (1994).
[8] P. A. Miller, G. A. Hebner, K. E. Greenberg, P. D. Pochan, and B. P. Aragon, J. Res. Natl. Inst. Stand. Technol. **100**, 427 (1995).
[9] Y. Wang, E. C. Benck, M. Misakian, M. Edamura, and J. K. Olthoff, J. Appl. Phys. **87**, (2000).
[10] B. Chapman, *Glow Discharge Processes* (J. Wiley, New York, 1980).
[11] J. K. Olthoff and Y. Wang, J. Vac. Sci. Technol. A **17**, 1552 (1999).
[12] For a discussion of quasistatic fields in capacitively coupled plasmas, see, for example, Y. P. Raizer, M. N. Schneider, and N. A. Yatsenko, *Radio-Frequency Capacitive Discharges* (Chemical Rubber, Boca Raton, FL, 1995).
[13] A. Schwabedissen, E. C. Benck, and J. R. Roberts, Phys. Rev. E **55**, 3450 (1997).
[14] Most of the data points shown in Fig. 3 are estimated by interpolating between the measured values reported by Miller *et al.*[8]
[15] M. Fivaz, S. Brunner, W. Schwarzenbach, A. A. Howling, and Ch. Hollenstein, Plasma Sources Sci. Technol. **4**, 373 (1995).
[16] In the Fivaz *et al.*[5] paper, x_s indicates the sheath width and d is related to the electric field associated with the presheath. Approximately the same interpretation can be given here if we think of the presheath region as extending far into the body of the plasma and that d does not completely characterize the presheath region.
[17] Because the plasma and the corresponding impedance continually changes during the pulsed excitation of the plasma, it is not possible for the matching network coupling the rf energy to the coil to be continually optimized. For the IED measurements reported in this article, the matching network was optimized for continuous excitation and the rf power value indicated is for the net power to the matching network driving the coil under continuous excitation.
[18] E. Benck, determined from measurement of optical emissions from argon plasma at 2.66 Pa (private communication).
[19] To achieve sufficient accuracy in the calculations for ions less than about 12 eV, the Δx value (9.5×10^{-5} cm) and the separation in X_o (26 μm) were reduced further.
[20] M. A. Sobolewski, J. K. Olthoff, and Y. Wang, J. Appl. Phys. **85**, 3966 (1999).
[21] F. W. Sears, *Thermodynamics, The Kinetic Theory of Gases, and Statistical Mechanics* (Addison–Wesely, Reading, MA, 1953).
[22] M. V. V. Rao, R. J. Van Brunt, and J. K. Olthoff, Phys. Rev. E **54**, 5641 (1996).
[23] J. Johannes, T. Bartel, G. A. Hebner, and J. Woodworth, J. Electrochem. Soc. **144**, 2448 (1997).
[24] A. E. Wendt, S.-B. Wang, and J. Werkling, Bull. Am. Phys. Soc. **44**, 10 (1999).